ISSN 1070-4272, Russian Journal of Applied Chemistry, 2019, Vol. 92, No. 3, pp. 360−366. © Pleiades Publishing, Ltd., 2019.
Russian Text © The Author(s), 2019, published in Zhurnal Prikladnoi Khimii, 2019, Vol. 92, No. 3, pp. 315−321.

MACROMOLECULAR COMPOUNDS AND POLYMERIC MATERIALS

Influence of the Molecular Polyimide Brush on the Gas Separation Properties of Polyphenylene Oxide

N. S. Tyan[a,]*, G. A. Polotskaya[a], T. K. Meleshko[a], A. V. Yakimansky[a], and Z. Pientka[b]

[a] *Institute of Macromolecular Compounds, Russian Academy of Sciences, St. Petersburg, 199004 Russia*
[b] *Institute of Macromolecular Chemistry, Czech Academy of Sciences, Prague, Czech Republic*
**e-mail: tyan-nadezhda91@yandex.ru*

Received October 18, 2018; revised November 26, 2018; accepted December 10, 2018

Abstract—A new hybrid gas separation membrane was prepared from poly(2,6-dimethyl-1,4-phenylene oxide) modified with graft copolyimide with side poly(methyl methacrylate) chains. The changes in the membrane structure on introducing up to 15 wt % modifier were evaluated by atomic force microscopy and density measurements. The microphase separation in modified polyphenylene oxide films was demonstrated. Introduction of graft copolyimide leads to an increase in the density of the hybrid films. The gas transport properties of the membranes were evaluated for H_2, CO_2, O_2, CH_4, and N_2. Introduction of up to 10 wt % modifier does not noticeably alter the permeability of the hybrid membranes to all the gases but increases the selectivity in gas separation.

Keywords: gas separation, membranes, graft copolyimides, selectivity, permeability

DOI: 10.1134/S1070427219030066

Membrane separation processes find increasing use in industry because they ensure high selectivity and allow organization of a continuous automated cost-saving process, easy integration into the existing flowsheets, and power saving [1–3]. These processes are characterized by simple implementation, low power consumption, low cost, high reliability, and high efficiency [4, 5].

One of the most promising ways to develop new membrane materials is modification of commercially produced polymers that exhibit high levels of heat resistance and mechanical properties in combination with satisfactory transport properties, but insufficient selectivity [6, 7]. Such polymers are modified with diverse inorganic [8–10] and polymeric [11–13] fillers. Recently there has been a great deal of interest in multicomponent polymer modifiers of complex architecture [14–16], allowing variation of the properties of the known commercial polymers in a wide range. Graft copolymers consisting of a backbone and of narrow dispersed side chains covalently bonded to it [16] can serve as such modifiers; they are termed polymer brushes [17–20].

Previously we prepared effective pervaporation membranes [21] from a film-forming regular graft copolymer with the polyimide (PI) backbone and narrow-dispersed poly(methyl methacrylate) (PMMA) side chains (hereinafter, PI–PMMA graft copolyimide). It seemed promising to use these graft copolyimides as a polymer modifier for gas separation membranes based on poly(2,6-dimethyl-1,4-phenylene oxide) (PPO). PPO is commercially produced and is used as a membrane component of a composite material in various membrane processes [22–26], including gas separation. In gas separation processes, PPO shows high permeability but low selectivity, which restricts its use [27–29]. Modification of the structure of PPO membranes with PI–PMMA can significantly influence the transport properties of the membrane. The structural formulas of the hybrid membrane components, (a) PPO and (b) PI–PMMA, are shown in the scheme.

This study was aimed at developing a procedure for preparing hybrid membranes based on polyphenylene oxide modified with graft copolyimide and at evaluating the effect of the modifier on the membrane structure

Scheme.

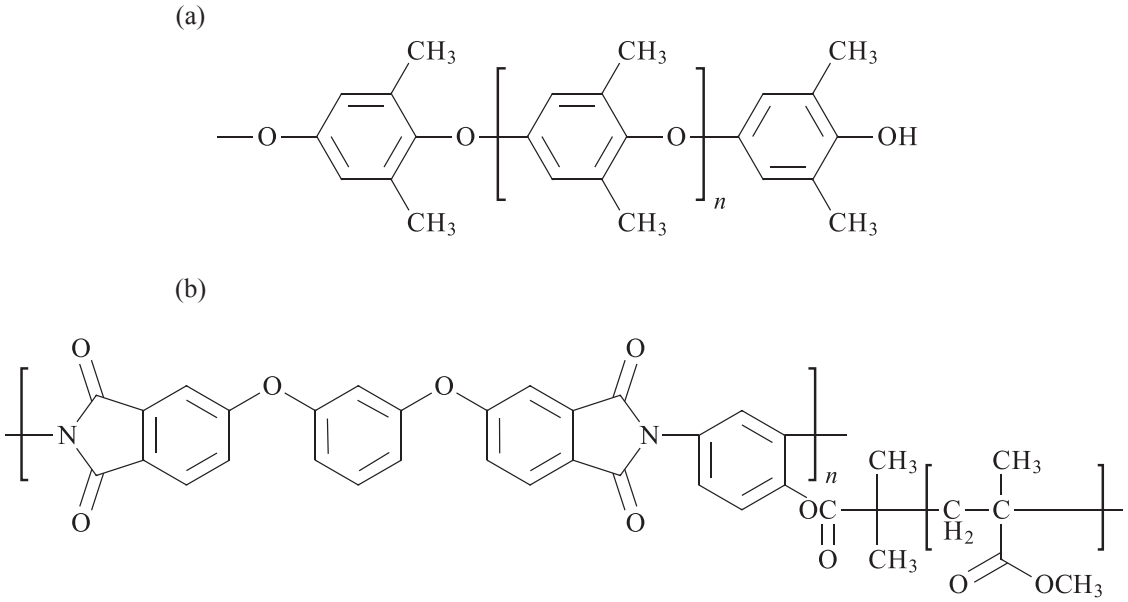

and its transport properties with respect to the gases H_2, CO_2, O_2, CH_4, and N_2.

EXPERIMENTAL

Materials. We used powdered poly(2,6-dimethyl-1,4-phenylene oxide) with MM ~ 338 kDa and the density $\rho = 1.054$ g cm^{-3} (Aldrich). Chloroform (Vekton, Russia, chemically pure grade) was used without additional purification. Samples of graft copolyimide, PI–PMMA, were prepared by MMA polymerization on a multifunctional polyimide macroinitiator (M_n = 35.2 × 10^3, M_w/M_n = 2.06, n = 52) by controlled atom transfer radical polymerization (ATRP) [30]. Grafting of PMMA chains to the PI chain was performed using AGET ATRP technique [31] as described in [32]. The density of grafting of PMMA side chains was 80%, and the mean degree of polymerization of side chains was m = 154 (M_n = 154.0 × 10^3, M_w/M_n = 1.4).

Membrane preparation. The PPO/PI–PMMA composites containing 5, 10, and 15 wt % PI–PMMA were prepared by mixing the individual solutions of PPO (3 wt %) and PI–PMMA (3 wt %) in chloroform using a power-driven stirrer. The polymer mixture solution was prepared by stirring for 60 min, followed by degassing. Membranes ~80–90 μm thick were prepared by casting the polymer mixture solution onto a smooth horizontal cellophane surface, which was followed by the solvent evaporation and vacuum drying at 40°C. Then the membrane was separated from the support and vacuum-dried at 40°C to constant weight.

Atomic force microscopy. Three-dimensional images of membrane surfaces were obtained using atomic force microscopy (AFM) with a Nanoscope III device (Digital Instruments, Santa Barbara, the United States) equipped with a 1553D scanner (Digital Instruments) in the tapping mode using OTESPA silicon cantilevers (Veeco Instruments, Dourdan, France) with the radius of 5 nm and vibration frequency of 300 kHz.

Determination of the membrane density. The membrane density ρ was determined at 25°C by the flotation method using an aqueous sucrose solution.

Gas separation. The permeability of H_2, CO_2, N_2, O_2, and CH_4 was measured by the barometric method using a high-vacuum laboratory apparatus and a cell with an effective area of 5.25 cm^2 at 30°C. The sample was kept in a vacuum in the cell for 50 h at 40°C, after which a gas was fed to the cell at a constant pressure p = 150 kPa. The gas permeability coefficient was determined from the pressure increase Δp_p in a calibrated volume V_p per the time interval Δt. The permeability coefficient P was calculated using the equation [33]

$$P = \frac{\Delta p_p}{\Delta t}\frac{V_p l}{Sp}\frac{1}{RT}, \quad (1)$$

where l is the membrane thickness; S, membrane area; T, temperature; and R, gas constant.

Effective diameters of gas molecules d_{eff} and characteristic values of the force constant of the Lennard–Jones potential $(\varepsilon/k)_{eff}$ [36]

Gas	d_{eff}, nm	$(\varepsilon/k)_{eff}$, K
H_2	0.210	62.2
O_2	0.289	112.7
N_2	0.304	83.0
CO_2	0.302	213.4
CH_4	0.318	154.7

The permeability coefficient was expressed in Barrers (1 Barrer = 10^{-10} $cm^3_{(STP)}$ cm cm^{-2} s cm^{-1} Hg). The ideal selectivity $\alpha_{i/j}$ of a membrane, reflecting its ability to separate one gas (i) from another (j), was calculated using the equation

$$\alpha_{i/j} = \frac{P_i}{P_j}, \quad (2)$$

where P_i is the permeability of gas i and P_j is that of gas j.

The diffusion coefficient D was calculated by the Daynes–Barrer method from the delay time θ [34, 35] using the equation

$$D = \frac{l^2}{6\theta}. \quad (3)$$

The solubility coefficient was calculated by the equation describing the gas transport [36]:

$$S = \frac{P}{D}. \quad (4)$$

The correlation analysis of the diffusion coefficients and gas solubility was performed using the data from the table.

RESULTS AND DISCUSSION

A series of hybrid membranes containing 5, 10, and 15 wt % PI–PMMA was prepared by varying the filler (PI–PMMA) content in the PPO matrix. An PPO membrane was prepared under similar conditions for comparison. Figure 1 shows the AFM images of the membrane surface relief. Uniformly distributed fluctuations of the membrane surface relief with the characteristic size from 50 to 100 nm can be seen in the AFM images of the hybrid membranes; these features suggest microphase separation in the polymer mixture, occurring apparently via precipitation of the graft copolyamide in the PPO matrix in the course of solvent removal during drying. An increase in the PI–PMMA content over 15 wt % led to the formation of defective membranes.

We have shown previously that the density of the membranes fabricated from PI–PMMA varied from 1.18 to 1.34 g cm^{-3} depending on the length of the side chains and on the density (thickness) of their grafting [21]. As PPO membranes have lower density (1.054 g cm^{-3}), introduction of filler of higher density into PPO led to the formation of hybrid membranes with the density higher than that of PPO (Fig. 2). The density of the hybrid membranes increased with an increase in the relative content of the graft copolyimide.

The transport properties of the membranes were studied at 30°C for the following gases: H_2, O_2, CO_2, CH_4, and N_2. Figure 3 shows dependence of the gas permeability coefficients on the concentration of the graft copolymer in the membranes. For all the samples, the gas permeability decreased in the order $H_2 > CO_2 > O_2 > CH_4 > N_2$. With an increase in the PI–PMMA content of the membranes, the permeability coefficient decreased for all the studied gases. This decrease was particularly noticeable at the PI–PMMA content higher than 10%.

Figure 4 shows the dependence of the selectivity for several ideal gas pairs on the content of the graft copolyimide in the membranes. An increase in the PI–PMMA concentration led to an increase in the selectivity. Appreciable increase was observed already with 5% filler. Introduction of larger (>5 wt %) amounts of the graft copolyimide into the matrix did not lead to a significant further increase in the selectivity for the gas pairs, but the permeability coefficient continued to appreciably decrease. The membrane with 5 wt % PI–PMMA showed good permeability and higher, compared to the PPO membrane, selectivity for the gas pairs, although the permeability coefficient somewhat decreased.

To study how changes in the composition and structure of PPO-based membranes after their modification with PI–PMMA influence the gas separation properties, we analyzed the constituents of the permeability coefficient

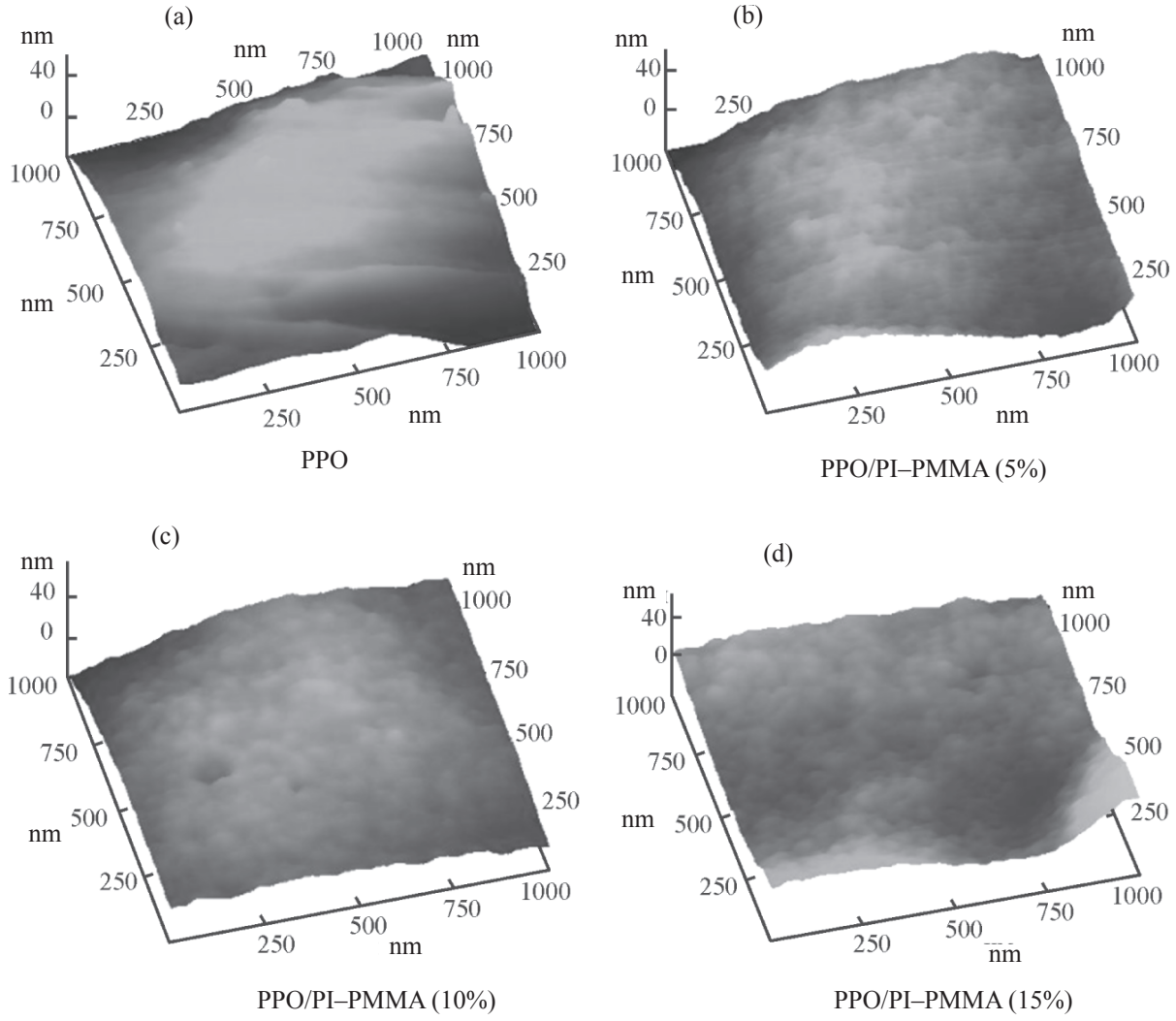

Fig. 1. AFM images of the surfaces of the (a) PPO and (b–d) PPO/PI–PMMA membranes.

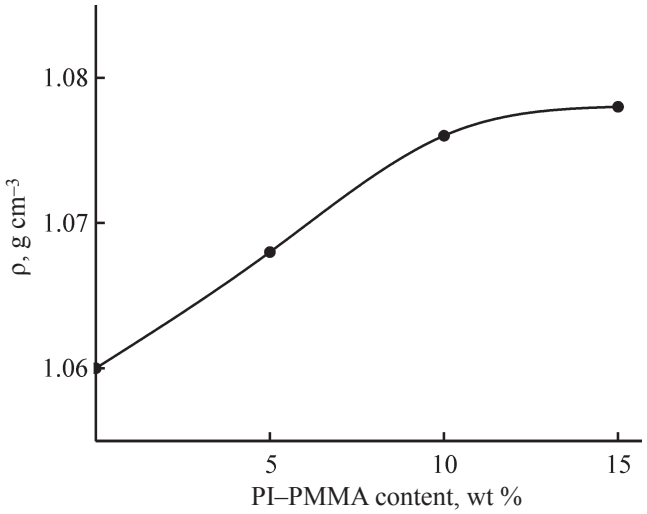

Fig. 2. Density of PPO/PMMA membranes ρ as a function of the PI–PMMA content.

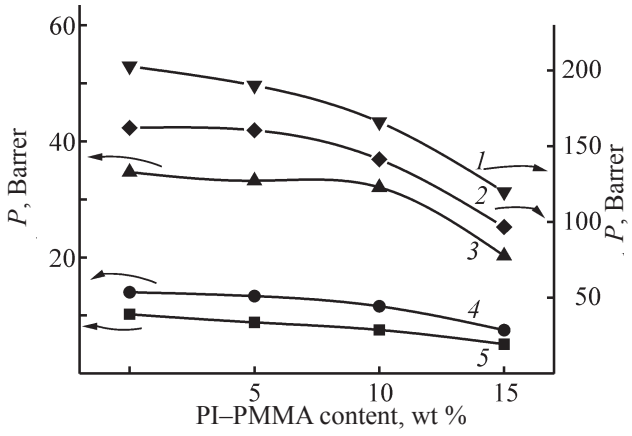

Fig. 3. Gas permeability coefficient P as a function of the PI–PMMA content in the membranes. Gas: (*1*) H_2, (*2*) CO_2, (*3*) O_2, (*4*) CH_4, and (*5*) N_2.

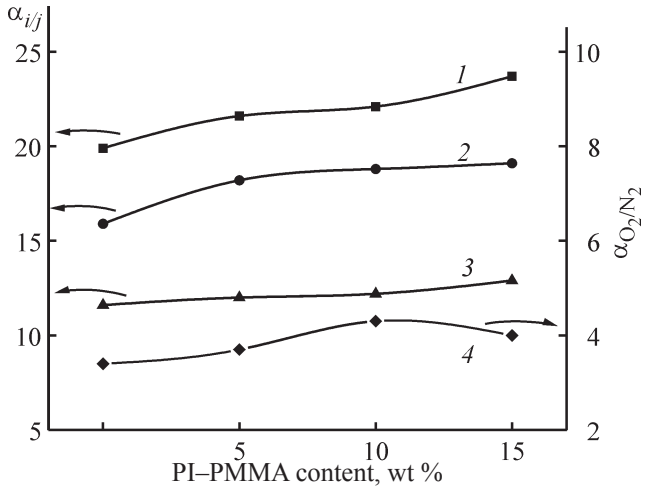

Fig. 4. Ideal selectivity $\alpha_{i/j}$ as a function of the PI–PMMA content of the membranes. Gas pairs: (*1*) H_2/N_2, (*2*) CO_2/N_2, (*3*) CO_2/CH_4, and (*4*) O_2/N_2.

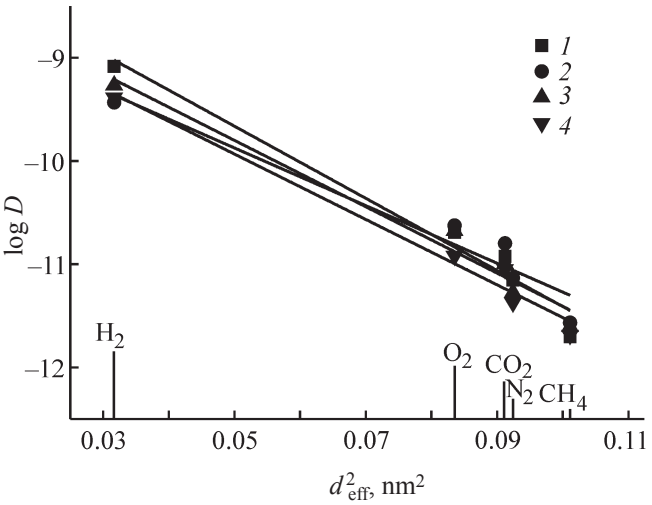

Fig. 5. Logarithm of the diffusion coefficient *D* as a function of the effective diameter of gas molecules squared, d^2_{eff}. Membrane: (*1*) PPO, (*2*) PPO/PI–PMMA(5%), (*3*) PPO/PI–PMMA(10%), and (*4*) PPO/PI–PMMA(15%).

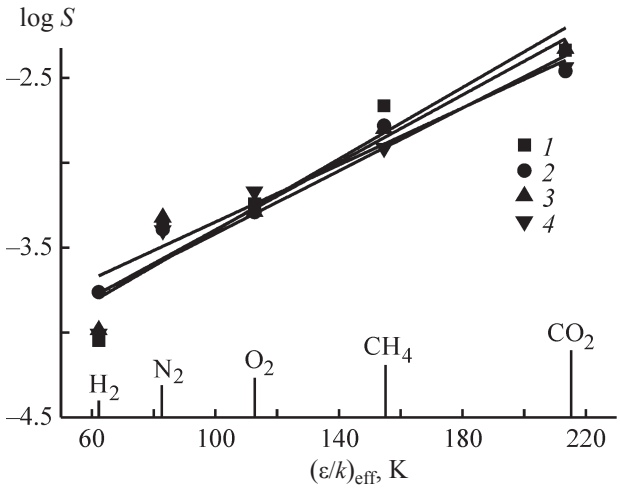

Fig. 6. Logarithm of the solubility coefficient *S* as a function of the Lennard–Jones force constant for gases $(\varepsilon/k)_{eff}$. Membrane: (*1*) PPO, (*2*) PPO/PI–PMMA(5%), (*3*) PPO/PI–PMMA(10%), and (*4*) PPO/PI–PMMA(15%).

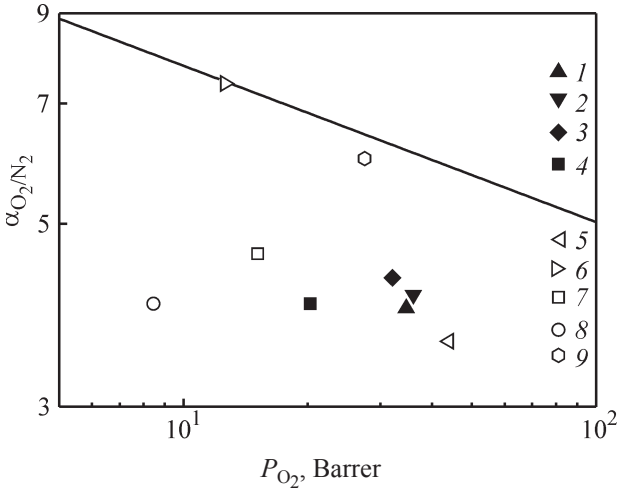

Fig. 7. Transport properties of the membranes (*1*) PPO, (*2*) PPO/PI–PMMA(5%), (*3*) PPO/PI–PMMA(10%), and (*4*) PPO/PI–PMMA(15%) in comparison with the published data for (*5*) Hs-PI-b-PVTMS-1 [40], (*6*) sulfonated brominated PPO (60% DBr, 32.9% DSul) [28], (*7*) 2% C60-PPO [41], (*8*) PPO-BzBr [42], and (*9*) MAgS800 [43], plotted on the Robeson diagram (selectivity α_{O_2/N_2} vs. permeability P_{O_2}) [39].

$P = DS$, namely, the diffusion coefficient D and the solubility coefficient S. The correlation analysis of the transport parameters for the polymer–gas system was performed by Teplyakov's method [37]. The basic correlation is the dependence of the diffusion coefficient on the effective diameter of the gas molecules. According to such approach [36], the experimental data on the diffusion coefficient should be fitted by a straight line in the coordinates $\log D = f(d^2_{eff})$, where d_{eff} is the effective diameter of the gas molecule. Figure 5 shows such dependence for PPO and PPO/PI–PMMA membranes. The linear dependence obtained for all the membranes confirms the reliability of the measurement results and indicates that the diffusion in the course of the gas separation mainly occurs via free volume in the polymer films.

Then, we studied dependence of the solubility coefficient on the force constant of the Lennard–Jones po-

tential for gases [36, 37]. This dependence should be linear in the coordinates $\log S = f(\varepsilon/k)_{\text{eff}}$, where $(\varepsilon/k)_{\text{eff}}$ is the characteristic value of the force constant of the Lennard–Jones potential. Figure 6 shows the plots for PPO and PPO/PI–PMMA membranes. The linear dependence obtained for the solubility coefficients confirms the reliability of the experimental data.

Comparison of the properties of the studied membranes with the known gas separation membranes. For objective evaluation of the performance of the membranes developed, we plotted the Robeson diagram [38, 39], i.e., the plot of the selectivity α_{O_2/N_2} vs. permeability coefficient P_{O_2}; the straight line shows the upper limit of the gas separation performance of all the membranes known by now. As seen from Fig. 7, the PPO membrane is one of the most selective membranes, and introduction of a modifier favors improvement of the selectivity of the PPO/PI–PMMA(10%) membrane. Thus, hybrid membranes containing graft copolyimides are perspective materials for preparation of gas separation membranes.

CONCLUSIONS

A hybrid membrane consisting of polyphenylene oxide and graft copolyimide with side poly(methyl methacrylate) chains was developed. It is characterized by increased density and relatively uniform heterophase structure, which is preserved upon incorporation of up to 15% graft copolyimide with side poly(methyl methacrylate) chains into the poly(2,6-dimethyl-1,4-phenylene oxide) matrix. Analysis of the transport properties of the membranes using the correlation dependences for the diffusion coefficients and gas solubility confirms the reliability of the gas permeability data obtained and indicates that the diffusion in the course of the gas separation mainly occurs via free volume in the polymer films. Introduction of the graft copolyimide with side poly(methyl methacrylate) chains increases the membrane selectivity; therefore, this modifier shows promise for gas separation membranes.

FUNDING

The study was supported by grant no. 14.W03.31.0022 (Megagrant of the Russian Federation Government).

REFERENCES

1. Baker, R.W., *Membrane Technology and Applications*, Chichester: Wiley, 2004.
2. Li, N.N., Fane, A.G., Winston, Ho W.S., and Matsuura, T., *Advanced Membrane Technology and Applications*, New Jersey: Wiley, 2008.
3. Salehi, F., *Food Bioprod. Process*., 2014, vol. 92, pp. 161–177.
4. Niknejad, S.M.S., Savoji, H., Pourafshari Chenar, M., and Soltanieh, M., *Int. J. Environ. Sci. Technol*., 2017, vol. 14, pp. 375–384.
5. Rybak, A., Dudek, G., Krasowska, M., Strzelewicz, A., and Grzywna, Z.J., *Sep. Sci. Technol*., 2014, vol. 49, pp. 1729–1735.
6. Liu, G., Xiangli, F., Wei, W., Liu, S., and Jin, W., *Chem. Eng. J*., 2011, vol. 174, pp. 495–503.
7. Yang, M., Zhao, C., Zhang, S., Li, P., and Hou, D., *Appl. Surf. Sci*., 2017, vol. 394, pp. 149–159.
8. Shames, A.I., Katz, E.A., Panich, A.M., et al., *Diam. Relat. Mater*., 2009, vol. 18, pp. 505–510.
9. Sun, H., Ma, C., Wang, T., Xu, Y., Yuan, B., Li, P., and Kong, Y., *Chem. Eng. Technol*., 2014, vol. 37, no. 4, pp. 611–619.
10. Sterescu, D.M., Stamatialis, D.F., Mendes, E., Wübbenhorst, M., and Wessling, M., *Macromolecules*, 2006, vol. 39, pp. 9234–9242.
11. Niang, M., Lu, G.S., and Schaetzel, P., *J. Appl. Polym. Sci*., 1997, vol. 64, no. 5, pp. 875–882.
12. Zhu, G.-Q., Gao, Q.-C., Li, Z.-H., Wang, F.-G., and Zhang, H., *Chem. Pap*., 2010, vol. 64, no. 6, pp. 776–782.
13. Vauclair, C., Tarjus, H., and Schaetzel, P., *J. Membr. Sci*., 1997, vol. 125, no. 2, pp. 293–301.
14. Polotskaya, G.A., Pulyalina, A.Y., Rostovtseva, V.A., Toikka, A.M., Saprykina, N.N., and Vinogradova, L.V., *Polym. Int*., 2016, vol. 65, no. 4, pp. 407–414.
15. Pulyalina, A.Y., Rostovtseva, V.A., Pientka, Z., Vinogradova, L.V., and Polotskaya, G.A., *Petrol. Chem*., 2018, vol. 58, no. 4, pp. 296–303.
16. Polotskaya, G.A., Lebedev, V.T., Pulyalina, A.Yu., and Vinogradova, L.V., *Petrol. Chem*., 2016, vol. 56, no. 10, pp. 925–936.
17. Grishin, D.F., *Polym. Sci., Ser. C*, 2011, vol. 53, no. 1, pp. 3–13.
18. Advincula, R.C., Brittain, W.J., Caster, K.C., and Rühe, J., *Polymer Brushes*, Weinheim: Wiley, 2004.
19. Zhang, M. and Müller, A.H.E., *J. Polym. Sci*., 2005, vol. 43, pp. 3461–3481.
20. Sheiko, S.S., Sumerlin, B.S., and Matyjaszewski, K.,

Prog. Polym. Sci., 2008, vol. 33, pp. 759–785.

21. Meleshko, T.K., Pulyalina, A.Yu., Tyan, N.S., Polotskaya, G.A., Ivanov, I.V., Kukarkina, N.V., Toikka, A.M., and Yakimansky, A.V., *Polym. Sci., Ser. B*, 2017, vol. 59, no. 2, pp. 183–193.
22. Chenar, M.P., Soltanieh, M., Matsuura, T., Tabe-Mohammadi, A., and Khulbe, K.C., *J. Membr. Sci*., 2006, vol. 285, pp. 265–271.
23. Polotskaya, G.A., Lebedev, V.T., Gofman, I.V., and Vinogradova, L.V., *Russ. J. Appl. Chem*., 2017, vol. 90, no. 9, pp. 1549–1557.
24. Penkova, A., Polotskaya, G., and Toikka, A., *Chem. Eng. Process*., 2015, vol. 87, pp. 81–87.
25. Kuznetsov, V.M., Toikka, A.M., Kuznetsov, Yu.P., Polotskaya, G.A., and Khripunov, A.K., *Russ. J. Appl. Chem*., 2004, vol. 77, no. 4, pp. 549–554.
26. Polotskaya, G.A., Gladchenko, S.V., Penkova, A.V., Kuznetsov, V.M., and Toikka, A.M., *Russ. J. Appl. Chem*., 2005, vol. 78, no. 9, pp. 1468–1473.
27. Polotskaya, G.A., Penkova, A.V., Toikka, A.M., Pientka, Z., Brozova, L., and Bleha, M., *Sep. Sci. Technol*., 2007, vol. 42, no. 2, pp. 333–347.
28. Hamad, F. and Matsuura, T., *J. Membr. Sci*., 2005, vol. 253, pp. 183–189.
29. Lee, H.-J., Suda, H., Haraya, K., and Moon, S.-H., *J. Membr. Sci.,* 2007, vol. 296, pp. 139–146.
30. Meleshko, T.K., Il'gach, D.M., Bogorad, N.N., Kukarkina, N.V., and Yakimansky, A.V., *Polym. Sci., Ser. B*, 2014, vol. 56, no. 2, pp. 118–126.
31. Ilgach, D.M., Meleshko, T.K., and Yakimansky, A.V., *Polym. Sci., Ser. C*, 2015, vol. 57, no. 1, pp. 3–19.
32. Meleshko, T.K., Ivanov, I.V., Kashina, A.V., Bogorad, N.N., Simonova, M.A., Zakharova, N.V., Filippov, A.P., and Yakimansky, A.V., *Polym. Sci., Ser. B*, 2018, vol. 60, no. 1, pp. 35–50.
33. Pientka, Z., Brozova, L., Pulyalina, A.Y., Goikhman, M.Y., Podeshvo, I.V., Gofman, I.V., Saprykina, N.N., and Polotskaya, G.A., *Macromol. Chem. Phys*., 2013, vol. 214, pp. 2867–2874.
34. Kryuchkova, S.V., Yablokova, M.Y., Gasanova, L.G., Kepman, A.V., and Alentiev, A.Y., *Moscow Univ. Chem. Bull.*, 2017, vol. 72, no. 3, pp. 120–127.
35. Yampolskii, Y., Alentiev, A., Bondarenko, G., Kostina, Y., and Heuchel, M., *Ind. Eng. Chem. Res*., 2010, vol. 49, no. 23, pp. 12031–12037.
36. Teplyakov, V.V. and Meares, P., *Gas. Sep. Purif*., 1990, vol. 4, pp. 66–78.
37. Malykh, O.V., Golub, A.Y., and Teplyakov, V.V., *Adv. Colloid Interface Sci*., 2011, vol. 164, nos. 1–2, pp. 89–99.
38. Robeson, L.M., *J. Membr. Sci.,* 1991, vol. 62, pp. 165–185.
39. Robeson, L.M., *J. Membr. Sci*., 2008, vol. 320, pp. 390–400.
40. Gacal, B.N., Filiz, V., Shishatskiy, S., Rangou, S., Neumann, S., and Abetz, V., *J. Polym. Sci.,* 2013, vol. 51, pp. 1252–1261.
41. Polotskaya, G., Biryulin, Yu., Pientka, Z., Brozova, L., and Bleha, M., *Fullerenes, Nanotubes Carbon Nanostruct*., 2004, vol. 12, nos. 1–2, pp. 365–369.
42. Bhole, Y.S., Kharul, U.K., Somani, S.P., and Kumbharkar, S.C., *Eur. Polym. J*., 2005, vol. 41, pp. 2461–2471.
43. Barsema, J.N., van der Vegt, N.F.A., Koops, G.H., and Wessling, M., *Adv. Funct. Mater*., 2005, vol. 15, pp. 69–75.